Schreurs, G., Hanni, R. and Vock, P. 2002. Analogue modelling of transfer zones in fold and thrust belts: a 4-D analysis. In: Schellart , W. P. and Passchier, C. W. 2002. Analogue modelling of large-scale tectonic processes. Journal of the Virtual Explorer , 7, 43-50.

Analogue modelling of transfer zones in fold and thrust belts: a 4-D analysis

GUIDO SCHREURS[1], RETO HÄNNI[1] & PETER VOCK[2]

[1] *Geological Institute, University of Bern, Baltzerstrasse 1, CH-3012 Bern, Switzerland,*
schreurs@geo.unibe.ch, www.earthsci.unibe.ch/people/schreurs/Main.htm
[2] *Institute for Diagnostic Radiology, Inselspital, CH-3010 Bern*

Abstract: We performed a series of analogue model experiments to investigate the development and evolution of transfer zones in fold and thrust belts. Experiments were done within the investigation field of a spiral computerized tomography (CT) scanner. This new-generation scanner revolves around the model and allows a 4-D analysis of the deforming model by generating time-lapse 3-D volumetric images. Computer visualisation techniques were used to create animations on the basis of CT images and to analyse 3-D geometry and kinematics of our models in detail. Granular materials were used to simulate the brittle behaviour of sediments, whereas a viscous Newtonian material was used to model the ductile flow of rock salt or other evaporites. Models showed a marked difference in structural evolution between domains that were underlain or not underlain by a thin viscous layer, representing brittle-viscous and brittle rheological domains, respectively. In the brittle domain, closely spaced and dominantly forward propagating thrusts formed a narrow and high fold-and-thrust belt. In the brittle-viscous domain, the thrust belt was wider and lower, and there was no consistent vergence of thrusting and folding. Transfer zones formed in the transition zone between the two domains. Location and orientation of these transfer zones are directly related to the geometry of the boundary between basal viscous layer and adjacent brittle layers. A lateral ramp formed where this boundary was initial parallel to the shortening direction, whereas an oblique ramp formed where this boundary was oblique. Both lateral and oblique ramps have a shallow dip and dip angles that change along strike. Thrusts in the brittle domain may propagate laterally into the brittle-viscous domain resulting in out-of-sequence thrusting. Experiments show that the location and orientation of transfer zones in nature may be controlled by rheological changes in the basal detachment.

Introduction

Three-dimensional structural changes along strike are commonly observed in fold and thrust belts. Examples have been documented e.g., in the western Salt Range of Pakistan (McDougall and Khan, 1990), in the Jura Mountains in France and Switzerland (Philippe, 1994, 1995; Philippe et al., 1998), and in the Alberta Foothills and Front Ranges of the Canadian Rocky Mountains (Fermor and Moffat, 1992; Fermor, 1999). Faults in such belts form part of a complex system of subhorizontal detachment faults, frontal ramps and transfer zones. The latter transfer displacement from one frontal ramp to the next. Transfer zones may be lateral ramps, oblique ramps or subvertical tear faults (McClay, 1992). The origins of transfer zones are diverse and can be related to, e.g., pre-existing basement faults, basal rheological changes, and variations in lithological thicknesses.

Analogue modeling experiments were performed to investigate the development and evolution of transfer zones. Transfer zones were induced by deforming a basal viscous layer that was placed adjacent to the mobile backstop and was overlain by brittle analogue materials. The shape of the basal viscous layer was varied in order to test its influence on the geometric and kinematic evolution of transfer zones. Experiments were analysed using helical (spiral) X-ray computerized tomography (CT; Hounsfield, 1973). This technique allows visualisation of the interior of an analogue model without destroying it. Periodic acquisition of volumetric data sets makes it possible to follow the three-dimensional evolution of the model structures at successive stage of deformation (Schreurs et al., in press). Results of experiments simulating transfer zones have been previously published by Schreurs et al. (2001). In this paper we focus on computer animations of these experiments that show in more detail the geometric and kinematic evolution of transfer zones.

Experimental procedure

The experimental apparatus consisted of a rectangular wooden box with a length of 80 cm, width of 43 cm and height of 17 cm. A vertical mobile backstop driven by a motor produced shortening at a constant velocity of 4.8 cm/h. A 5 mm thick layer of viscous polydimethyl-siloxane (PDMS; viscosity of 5×10^4 Pa s, Weijermars, 1986) was placed over part of the wooden base (Fig. 1). Granular, brittle analogue materials (dry quartz sand and corundum powder with an average grain size of 100 μm) were sprinkled in alternate layers on top of the PDMS and the adjacent uncovered wooden base. The initial model was 80 cm long, 27 cm wide, and its thickness was 3 cm. Total shortening amounted to 9 cm, reducing the final model width to 18 cm. Three-dimensional CT data sets were obtained from part of the initial, undeformed model (Fig. 1) and subsequently after every full centimeter of progressive shortening, giving a total of ten three-dimensional data sets. From the three-dimensional volume raw data, 88 (experiment 73) and 74 (experiment 75) cross-sectional slices with 2 mm spacing were computed retrospectively. Thus, the field of investigation width covered 17.6 and 14.8 cm, respectively. The computed attenuation values of each cross-sectional slice resulted in a grey scale image. Digital data were stored on CD-Rom

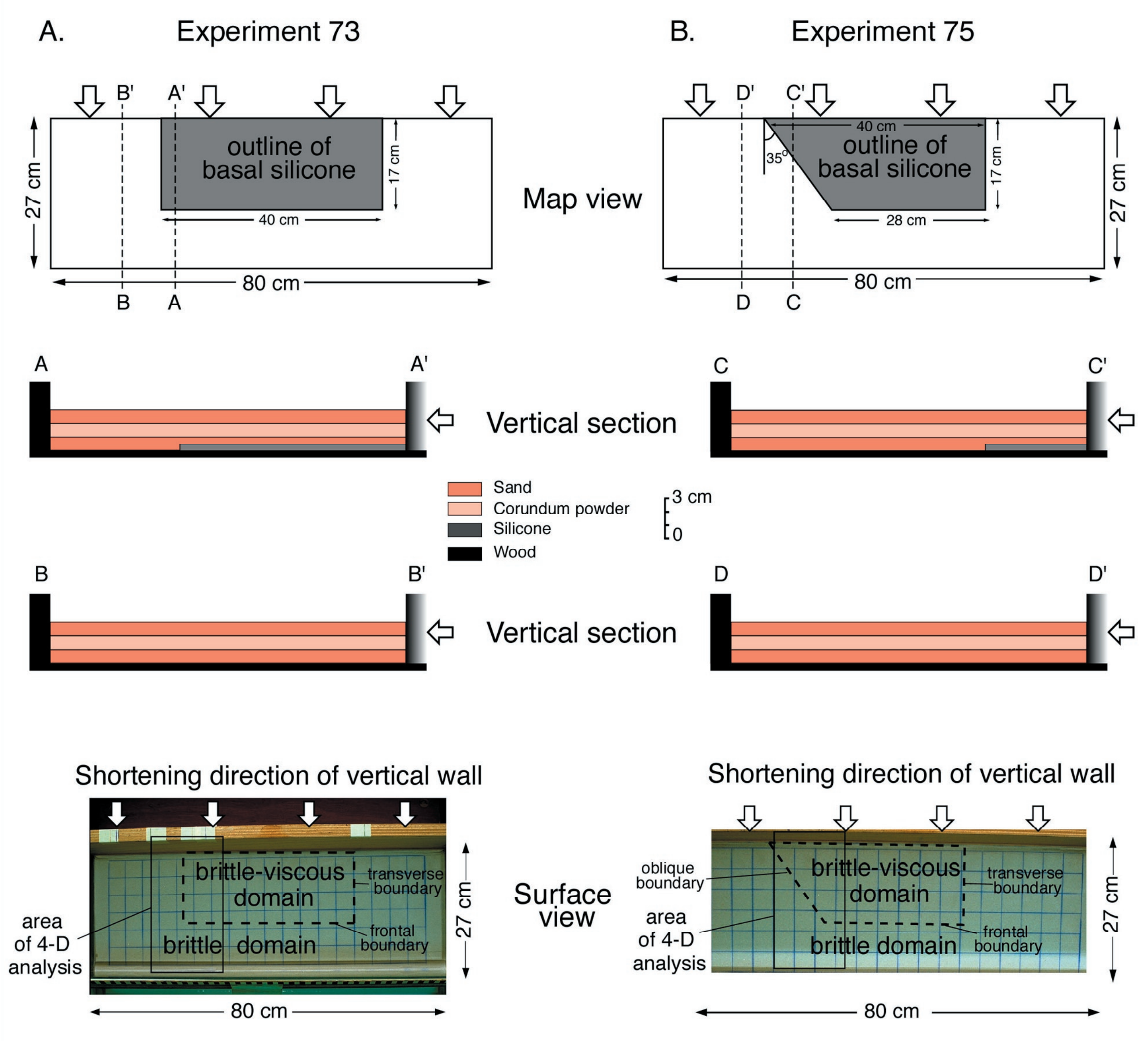

Figure 1. Initial experimental setup illustrated by map view, vertical sections and surface photographs. (a) Experiment 73. (b) Experiment 75. Boundary conditions were identical except for the shape of the basal layer of viscous polydimethylsiloxane (PDMS), whose initial outline is indicated by a dashed line. Area analysed by X-ray computerized tomography (CT) is shown on plan view photographs. Initial grid spacing of model is 5 cm.

in Dicom 3.0 standard format ensuring interoperability with visualisation software. NIH image software was used to enhance images and to produce movies of serial cross-sections through one particular deformation stage or the time evolution of model deformation in two dimensions. Noesys T3D visualisation software was used to generate 3-D perspective views from serial cross-sections. This software also provides the possibility to compute sections in any direction through a three-dimensional data set, i.e., cross, longitudinal, oblique, or horizontal sections. Three-dimensional views at successive deformation stages were used to make short movies.

Experiments

We show the results of two experiments with identical boundary conditions, except for the shape of the basal layer of viscous PDMS (Fig. 1). In experiment 73 the model had two lateral PDMS-sand boundaries parallel to, and one frontal boundary perpendicular to, the shortening direction (Fig. 1a). In experiment 75, one side of the PDMS layer was oblique to the shortening direction (at an angle of 35°), while the other side was parallel to it (Fig. 1b). Purely for descriptive purposes we refer to the sand-corundum-sand layers as the brittle domain, and to the sand-corundum-sand layers with a basal viscous PDMS layer as the brittle-viscous domain. In both experiments the structural evolution in the brittle domain differed markedly from the one in the brittle-viscous domain. X-ray CT volumetric data were acquired from the area indicated in Fig. 1.

Experiment 73 – Evolution of structures in cross-sections through the brittle and brittle-viscous domain

Progressive shortening was initially accommodated by thrust faults with opposite vergence (Fig. 2). The downward converging thrust faults defined a pop-up structure that rooted near the base of the lowermost sand layer in the brittle domain and at the top of the viscous layer in the brittle-viscous domain. The backthrusts dip

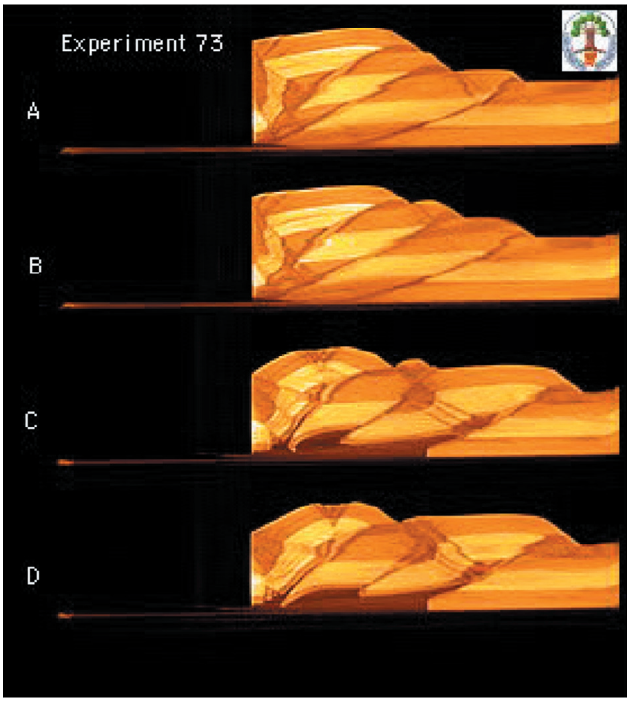

Figure 2. Movie of cross-sectional evolution of experiment 73 illustrating the difference in structural style between brittle and brittle-viscous domain. Each section represents a 2 mm thick X-ray computerized tomography (CT) slice that was acquired parallel to the shortening direction. The upper two sections in each frame cross the brittle domain, the lower two sections the brittle-viscous domain. Initial width of the model was 27 cm; initial height was 3 cm. Shortening increment between frames is 1 cm. PDMS = dark brown, sand = light brown, corundum powder = yellow. **(Select image to view movie)**

steeper than the forward thrusts. As deformation increased, forward thrusts were predominantly active. Backthrusts showed little movement and were passively transported over the forward thrust. Fault-bend folds formed as the thrust sheet moved over the ramp of the forward thrust. In the brittle-viscous domain, viscous material moved upward along the ramp.

In the brittle domain, progressive deformation caused the basal detachment to be activated in front of the pop-up structure and a new thrust imbricate formed. Activity along the older forward thrust ceased and fault movement began to occur along the newly developed forward thrust in its footwall. With increasing deformation, another in-sequence imbricate thrust formed.

In the brittle-viscous domain, however, progressive deformation resulted in the development of a new frontal thrust far away from the mobile wall at the forward boundary between basal PDMS and sand. Displacement along the forward thrust of the pop-up structure near the mobile wall ceased. Because of continuing movement of the mobile wall, the forward thrust of the pop-up became progressively steeper and the triangular block bounded by forward thrust, backthrust and mobile wall underwent a rotation about a horizontal axis. This boundary effect caused bulging and extension in the upper part of the fault-bend fold and small normal faults formed in its outer arc. As progressive shortening increased, backthrusts formed at the lower bend of the active frontal ramp in the brittle-viscous domain. In this domain, an out-of-sequence thrust appeared in the region between the existing forward thrusts. Movement along the out-of-sequence thrust took

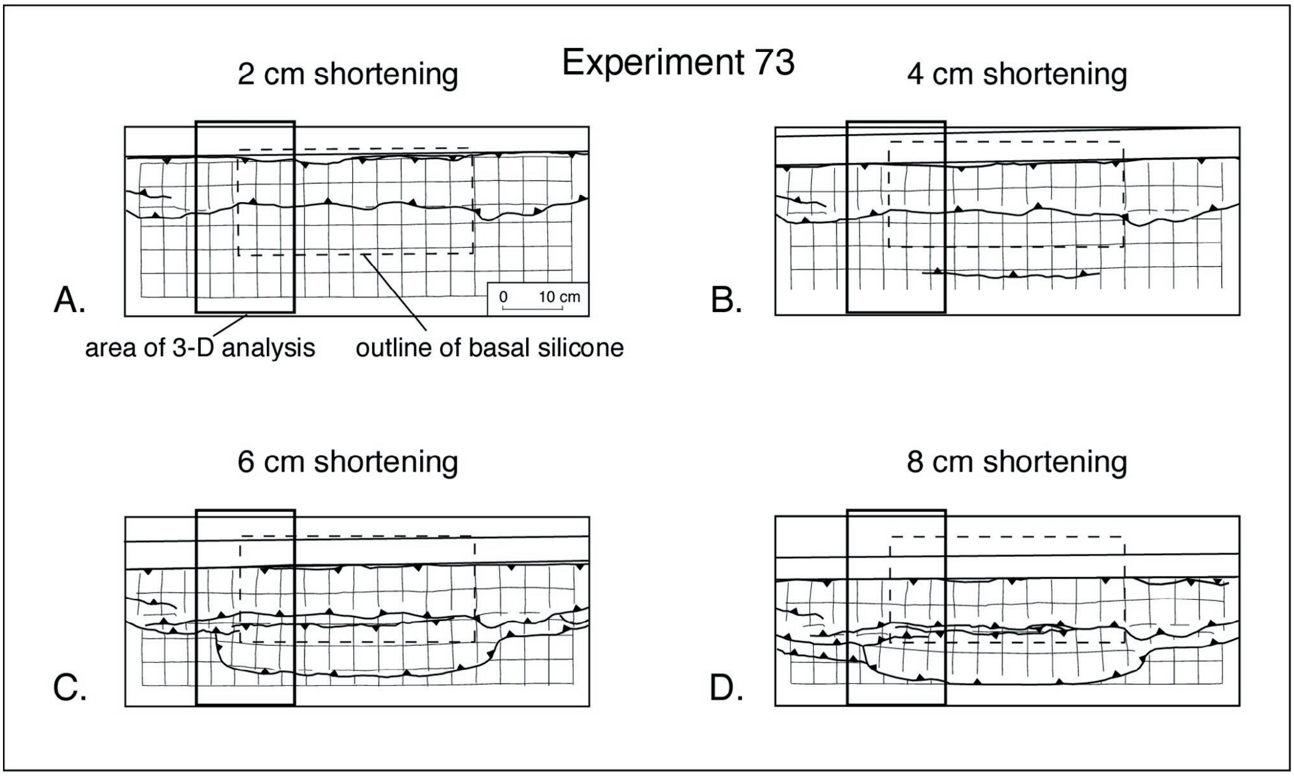

Figure 3. Line drawings after plan view photographs of experiment 73 illustrating progressive development of surface structures at 2, 4, 6 and 8 cm of shortening. Transfer zones connecting frontal ramps develop parallel to the shortening direction.

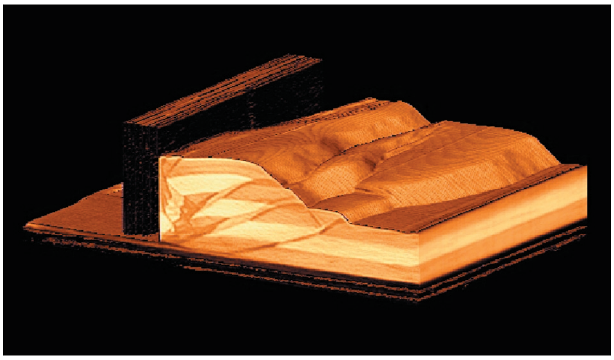

Figure 4. Movie of 3D evolution with time of experiment 73 illustrating the formation of a transfer zone. Each frame shows a perspective three-dimensional view that consists of 88 serial cross-sections each representing a 2 mm thick CT slice. Brittle domain closest to viewer. Initial width and height of the model was 27 cm and 3 cm, respectively. Shortening increment between frames is 1 cm. **(Select image to view movie)**

Figure 5. Movie of 3D evolution with time of experiment 73 illustrating the formation of a transfer zone. Each frame shows a perspective three-dimensional view that consists of 88 serial cross-sections each representing a 2 mm thick CT slice. Brittle-viscous domain closest to viewer. Shortening increment between frames is 1 cm. **(Select image to view movie)**

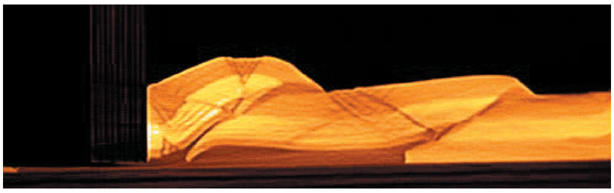

Figure 6. Movie illustrating the geometry of part of the model (experiment 73) by a series of serial vertical sections at 6 cm shortening. Note how the active frontal thrust in the brittle domain propagates laterally into the brittle-viscous domain where it represents an out of sequence thrust that is active at the same time as the pop-up structure that formed at the frontal sand-PDMS boundary. Computer animation shows 88 frames at 3 frames per second. The lateral ramp defining the transfer zone is visible in frames between t = 9 seconds and t = 12 seconds. **(Select image to view movie)**

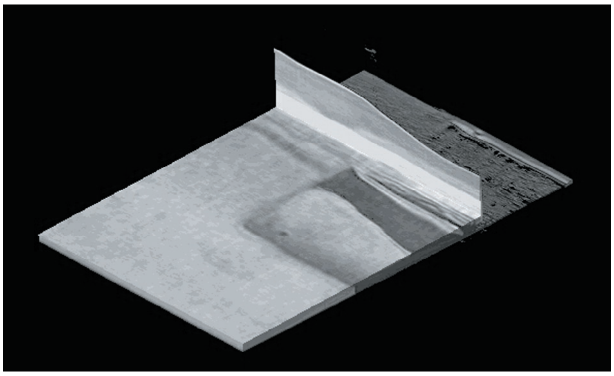

Figure 7. Movie showing cut-out 3D views of experiment 73 at 7 cm shortening. The longitudinal sections through the 3D views show clearly that the lateral ramp roots at the basal viscous layer and has a shallow dip (< 30°). PDMS = dark grey, sand = medium grey, corundum powder = light grey. **(Select image to view movie)**

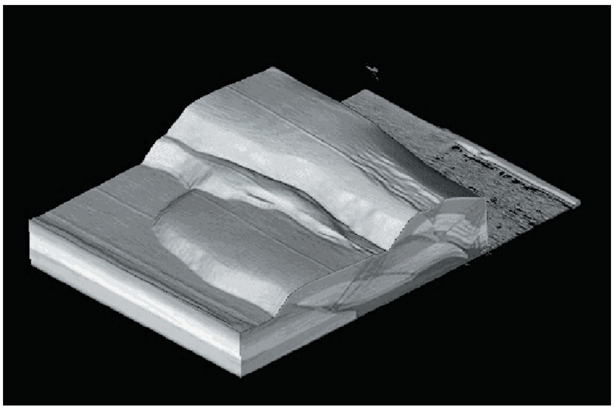

Figure 8. Movie showing cut-out 3D views of experiment 73 at 7 cm shortening. The horizontal sections show the curvature of the thrust front and how backthrusts die out along strike as they approach the transfer zone. **(Select image to view movie)**

place at the same time as displacement along the foremost forward thrust. Displacement along this out-of-sequence thrust was also coeval with movement along backthrusts of the frontal pop-up structure and resulted in a complex interference pattern.

Experiment 73 in surface view and the development of a transfer zone

In surface view, thrust faults developed first in the brittle domain and propagated along strike into the brittle-viscous domain. Downward-converging thrust faults bound a pop-up structure that strikes parallel to the mobile wall (Fig. 3). Since forward thrusts in the brittle-viscous domain rooted at the top of the viscous layer and dipped slightly steeper than in the brittle domain, the thrust front surfaced slightly closer to the mobile wall in the brittle-viscous domain (Fig. 3a). With progressive shortening, a forward thrust originated at the frontal boundary between brittle and viscous material (Fig. 3b). Deformation then took place in two completely different parts of the model: close to the mobile wall in the brittle domain, and near the frontal termination of the basal PDMS in the brittle-viscous domain. (Fig. 3c,d).

The frontal thrusts linked up along transfer zones that formed subparallel to the shortening direction (Fig. 3c). Figures 4 and 5 show the 3D evolution of a transfer zone from two different perspectives. Note that the thrust imbricate that formed in the brittle domain in the footwall of the pop-up structure propagated laterally into the brittle-viscous domain and caused the out-of-sequence thrust in the latter domain (as seen in cross-sections; Fig. 2 & 5). The 3D geometry of the transfer zone (after 6 cm shortening) is illustrated by serial vertical cross-sections (Fig. 6). In longitudinal sections parallel to the mobile wall, the fault defining the transfer zone rooted at the sand-PDMS boundary and had a listric shape (Fig. 7). This fault is a lateral ramp striking subparallel to the shortening direction. The dip of the lateral ramp decreased along strike toward the frontal ramp in the brittle-viscous domain, from about 30° to less than 10° (Fig. 7). In horizontal sections through the transfer zone, the curvature of the thrust front is clearly visible (Fig. 8). These sections also show how the backthrust of the frontal pop-up dies out along strike as it approaches the transfer zone. In the area of the transfer zone, coeval movement occurred along several thrusts, whereas fault activity in the brittle domain was restricted to the foremost forward thrust (Fig. 4 & 5). As a consequence, the initially curved geometry of the thrust front in surface view became less pronounced with progressive shortening (see final stages of Fig. 4 & 5).

Experiment 75

In this experiment one boundary of the basal viscous layer was oblique and made an angle of 35° with the shortening direction (Fig. 1b). The initial evolution of structures was similar to that in the previous experiment. A pop-up structure formed close to the mobile wall (Fig. 9a). As deformation increased, in-sequence imbricate thrusts developed in the brittle domain, while a new pop-up structure formed in the brittle-viscous domain. That structure formed far away from the mobile wall at the frontal boundary between sand and PDMS (Fig. 9b). With progressive shortening, the less advanced thrusts linked up with the farther advanced thrusts by means of transfer zones (Fig. 9c). In contrast to the previous

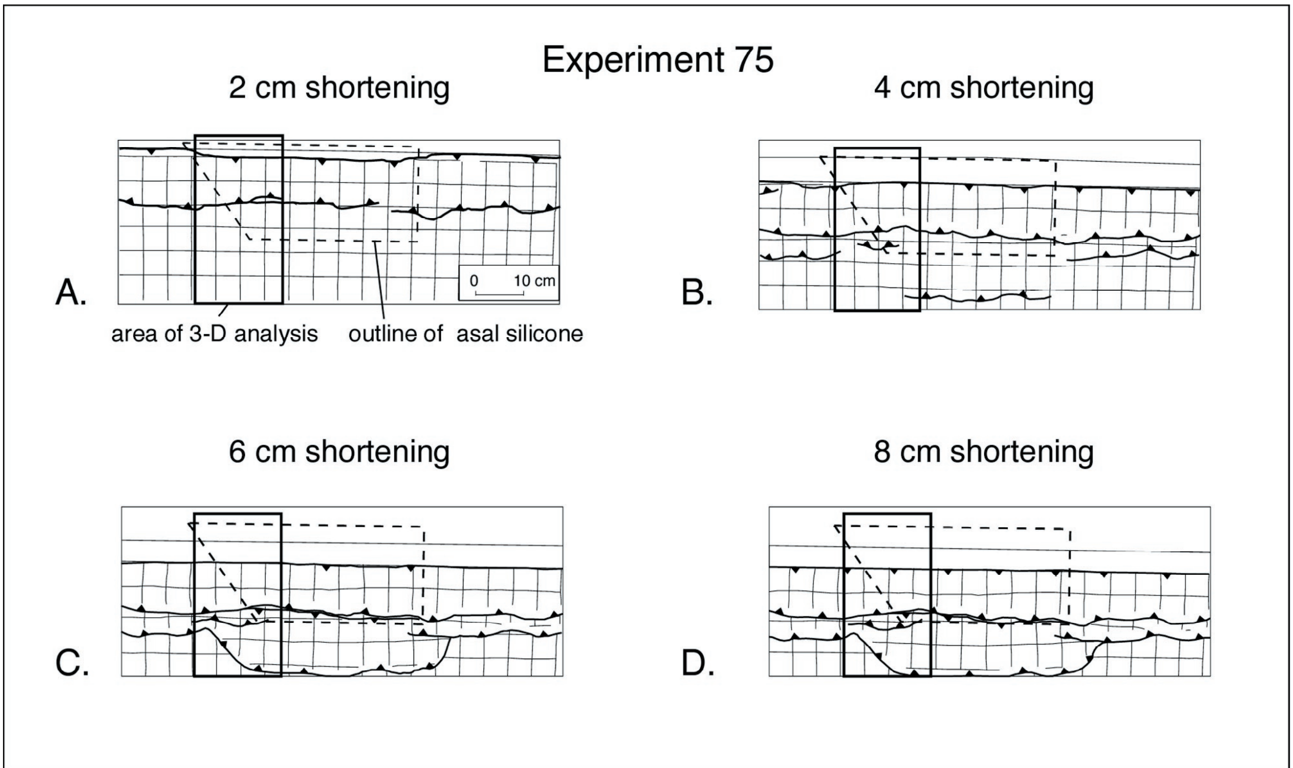

Figure 9. Line drawings after plan view photographs of experiment 75 illustrating progressive development of surface structures at 2, 4, 6 and 8 cm of shortening. Transfer zones connecting frontal ramps develops oblique to the shortening direction.

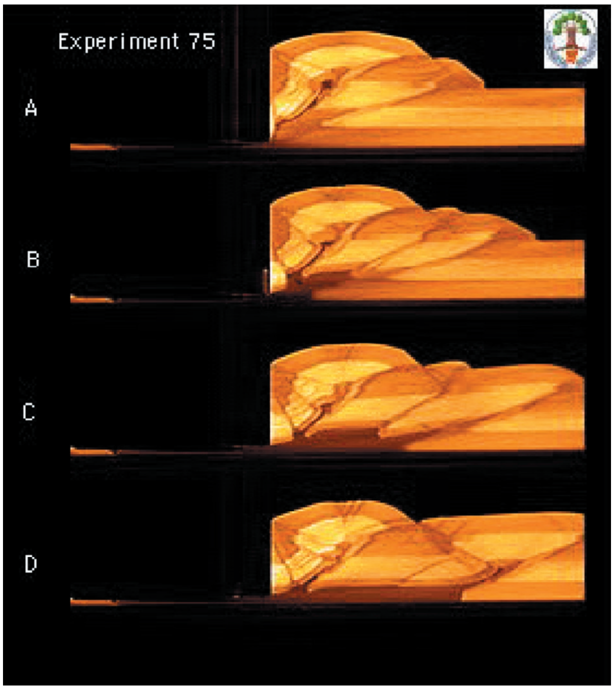

Figure 10. Cross-sectional evolution of experiment 75. Each section represents a 2 mm thick X-ray computerized tomography (CT) slice that was acquired parallel to the shortening direction. Initial width of the model was 27 cm; initial height was 3 cm. Shortening increment between frames is 1 cm. **(Select image to view movie)**

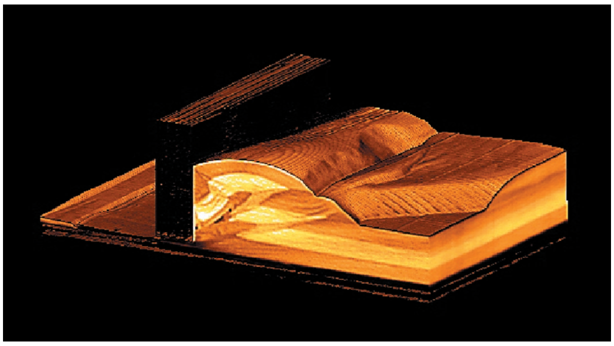

Figure 11. Movie of 3D evolution with time of experiment 75 illustrating the formation of a transfer zone striking oblique to the shortening direction. Each frame shows a perspective three-dimensional view that consists of 74 serial cross-sections each representing a 2 mm thick CT slice. Brittle domain closest to viewer. Initial width and height of the model was 27 cm and 3 cm, respectively. Shortening increment between frames is 1 cm. **(Select image to view movie)**

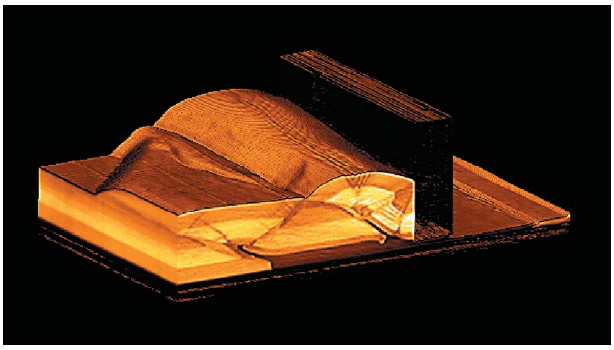

Figure 12. Movie of 3D evolution with time of experiment 75 illustrating the formation of a transfer zone. Each frame shows a perspective three-dimensional view that consists of 74 serial cross-sections each representing a 2 mm thick CT slice. Brittle-viscous domain closest to viewer. Shortening increment between frames is 1 cm. **(Select image to view movie)**

Figure 13. Movie illustrating the geometry of part of the model (experiment 75) by a series of serial vertical sections at 6 cm shortening. Note how the active frontal thrust in the brittle domain propagates laterally into the brittle-viscous domain. Computer animation shows 74 frames at 3 frames per second. **(Select image to view movie)**

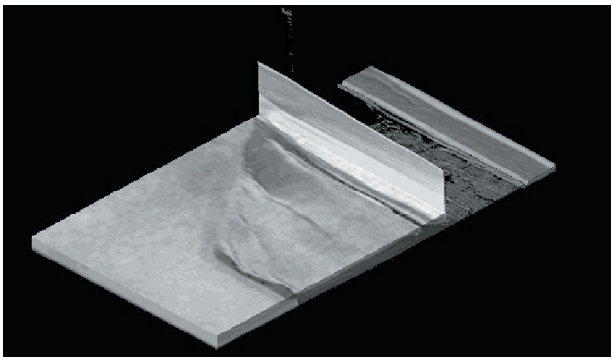

Figure 14. Movie showing cut-out 3D views of experiment 75 at 7 cm shortening. The longitudinal sections through the 3D views show clearly that the oblique ramp roots at the basal viscous layer and has a shallow dip (< 30°). **(Select image to view movie)**

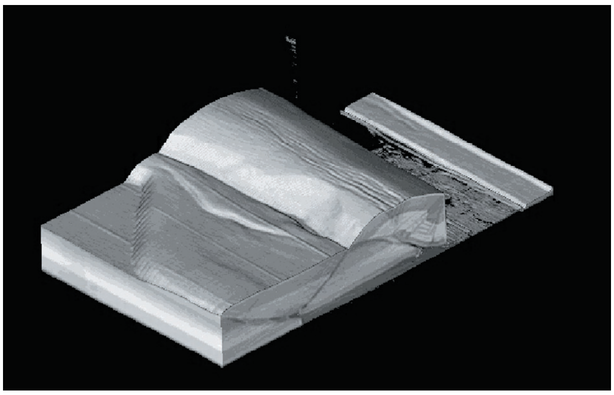

Figure 15. Movie showing cut-out 3D views of experiment 75 at 7 cm shortening. The horizontal sections show the curvature of the thrust front and how backthrusts die out along strike as they approach the transfer zone. **(Select image to view movie)**

experiment, however, the transfer zone underlain by the oblique trending sand-PDMS boundary developed a strike oblique (35°) to the shortening direction (Fig. 9c, d). Fig. 10 shows the evolution in cross-section through the brittle-viscous domain. As in the previous experiment, a forward thrust that formed in the brittle domain propagated along strike into the brittle-viscous domain (Fig. 10). This thrust was active at the same time as the most frontal thrust located at the frontal PDMS-sand boundary (Fig. 10). The 3D evolution of the oblique transfer zone is shown from different perspectives in Fig. 11 & 12. The geometry of the transfer zone is illustrated by serial vertical cross-sections at 6 cm shortening (Fig. 13). Perspective 3D views reveal the geometry of the oblique ramp (Fig. 14 & 15; at 7 cm shortening). The maximum dip of the transfer zone was 30° and decreased along strike toward the frontal ramp. Backthrusts of the frontal pop-up structure in the brittle-viscous domain die out along strike in the brittle domain.

Conclusions

The experiments showed a contrast in structural evolution between domains underlain and not underlain by a thin viscous PDMS layer. Thrust faults in the brittle domain were closely spaced and a narrow and high fold and thrust belt formed. The sequence of thrusting propagated forward and the belt had a dominant vergence of thrusts and associated folds. In the brittle-viscous domain, however, spacing between thrusts was greater and the fold and thrust belt was wider and lower. A frontal pop-up structure formed at the frontal sand-PDMS boundary. There was no consistent vergence of thrusts and folds in the brittle-viscous domain. Transfer zones formed in the transition zone between brittle and brittle-viscous domains. Out of sequence thrusting and coeval activity of different thrusts occurred in the brittle-viscous domain close to where the transfer zone developed. This resulted from along-strike propagation of forward thrusts from the brittle domain into the adjacent brittle-viscous domain. Location and orientation of transfer zones was directly related to the basal geometry of the viscous layer. Transfer zones rooted in the viscous layer and their strike closely mimicked the orientation of the basal boundary between viscous and brittle material. A lateral ramp formed where this boundary was parallel to the shortening direction, whereas an oblique ramp formed where this boundary was oblique.

Our experiments suggest that salt or other rheologically weak layers at the base of a sedimentary sequence may favour out of sequence thrusting and coeval displacement along different forward thrusts in areas closely adjacent to transfer zones. The location and orientation of transfer zones in nature may be controlled by basal rheological changes. Lateral and oblique ramps in transfer zones may have shallow dips (<30°) and dip angles that vary along strike. Backthrusts of frontal pop-up structures in areas underlain by rheologically weak layers may interfere with forward thrusts that formed in purely brittle domains, thus contributing to the complexity of transfer zones in nature.

Acknowledgments

Funding by Hochschulstiftung Bern and Swiss National Science Foundation Grant 2000-0554.11 98/1 is gratefully acknowledged. Andrea Schneider and Cindy Seiler are thanked for assistance in computerized tomography data acquisition, and Hans-Peter Bärtschi for technical assistance.

References

Fermor, P. R., and Moffat, I. W., 1992, Tectonics and structure of the western Canada Foreland Basin, in Macqueen, R. W., and Leckie, D. A., eds., Foreland basins and fold belts: Tulsa, Oklahoma, American Association of Petroleum Geologists, Memoir 55, p. 81-105.

Fermor, P., 1999, Aspects of the three-dimensional structure of the Alberta Foothills and Front Ranges: Geological Society of America Bulletin, v. 111, p. 317-346.

Hounsfield, G. N., 1973, Computerized transverse axial scanning (tomography): British Journal of Radiology, v. 46, p. 1016-1022.

McClay, K. R., 1992, Glossary of thrust tectonics terms, in McClay, K. R., ed., Thrust tectonics: London, Chapman & Hall, p. 419-433.

McDougall , J. W., and Khan, S. H., 1990, Strike-slip faulting in a foreland fold-thrust belt: the Kalabagh Fault and western Salt Range, Pakistan: Tectonics, v. 9, p. 1061-1075.

Philippe, Y., 1994, Transfer zone in the southern Jura thrust belt (eastern France): geometry, development and comparison with analogue modelling experiments, in Mascle, A., ed., Hydrocarbon and petroleum geology of France: European Association of Petroleum Geologists, no. 4, p. 327-346.

Philippe, Y., 1995, Rampes latérales et zones de transfert dans les chaînes plissées: géometrie, conditions de formations et pièges structuraux associés [Ph.D. thesis]: Université de Savoie, France, 623 p.

Philippe, Y., Deville, E., and Mascle, A., 1998, Thin-skinned inversion tectonics at oblique basin margins: example of the western Vercors and Chartreuse Subalpine massifs (SE France), in Mascle, A., Puigdefabregas, C., Luterbacher, H. P., and Fernandez, M., eds., Cenozoic Foreland Basins of Western Europe: Geological Society London, Special Publications, v. 134, p. 239-262.

Schreurs, G., Hänni, R., Panien, M. & Vock, P. (in press). Analysis of analogue models by helical X-ray computerized tomography. In: Jacobs, P. (ed.). Applications of computerised X-ray tomography in geology and related domains. Geological Society London, Special Publications

Schreurs, G., Hänni, R. & Vock, P. (2001). 4-D Analysis of analog models: Examples of transfer zones in fold-and-thrust belts. In: Koyi, H.A. & Mancktelow, N.S. (eds.): Tectonic modeling: A volume in honor of Hans Ramberg, Geological Society of America Memoir 193, p. 179-190.

Weijermars, R., 1986, Flow behaviour and physical chemistry of bouncing putties and related polymers in view of tectonic laboratory applications: Tectonophysics, v. 124, p. 325-258.